A Letters Journal Exploring the Frontiers of Physics

February 2010

EPL, **89** (2010) 34004
doi: 10.1209/0295-5075/89/34004

www.epljournal.org

Analogue gravity and ultrashort laser pulse filamentation

D. Faccio[1,2(a)], S. Cacciatori[2], V. Gorini[2], V. G. Sala[1,2], A. Averchi[1,2], A. Lotti[1,2], M. Kolesik[3] and J. V. Moloney[3]

[1] *CNISM - Via della Vasca Navale 84, I-00146, Rome, Italy, EU*
[2] *Department of Physics and Mathematics, Università dell'Insubria - Via Valleggio 11, I-22100 Como, Italy, EU*
[3] *Arizona Center for Mathematical Sciences and Optical Sciences Center, University of Arizona Tucson, 85721 AZ, USA*

received 25 November 2009; accepted in final form 21 January 2010
published online 19 February 2010

PACS 42.65.Jx – Beam trapping, self-focusing and defocusing; self-phase modulation
PACS 04.70.Dy – Quantum aspects of black holes, evaporation, thermodynamics

Abstract – Ultrashort laser pulse filaments in dispersive nonlinear Kerr media induce a moving refractive index perturbation which modifies the spacetime geometry as seen by co-propagating light rays. We study the analogue geometry induced by the filament and show that one of the most evident features of filamentation, namely conical emission, may be precisely reconstructed from the geodesics. We highlight the existence of favorable conditions for the study of analogue black hole kinematics and Hawking-type radiation.

The persistent lack of a satisfactory quantum model of gravity has led to the development of a semiclassical approach in which the dynamics of a quantum field is analyzed in the curved-spacetime metric determined by the classical gravitational field [1]. One of the most intriguing predictions of the semiclassical model is the thermalization of the quantum field in the presence of the event horizon of a black hole [2]. However, it turns out that for a typical stellar mass black hole the temperature of this expected radiation is so low ($\sim$10 nK) and the intensity of the latter far away from the actual source is so weak as to be extremely unlikely to ever be detected. On the other hand, Unruh proposed the use of gravity analogue systems that reproduce the kinematics of gravitational systems as a means to gain insight and experimental verification of gravitational theories in Earth-based laboratories [3]. A number of analogue systems have been proposed, relying mainly on acoustic perturbations in low-temperature condensates and on light rays in a moving dielectric [4,5]. These mostly suffer from the same limitation of astrophysical black holes, *i.e.* extremely low Hawking temperatures, and therefore continue to pose a strong experimental challenge. More recently Philbin *et al.* proposed a dielectric medium based analogue in which a fiber soliton generates, through the nonlinear Kerr effect, a refractive index perturbation (RIP) which modifies the spacetime geometry as seen by co-propagating light rays [6]. The Hawking temperature in the laboratory reference frame is found to be given by $kT = \hbar\alpha/2\pi c$, where the surface gravity $\alpha = -(c/\delta n)\partial\delta n/\partial\tau$ is determined by the variation of the RIP along the retarded-time coordinate τ.

Ultrashort laser pulse filamentation in bulk dispersive media with Kerr nonlinearity is characterized by the transformation of an input bell-shaped laser pulse into a tightly focused, high-intensity peak that may propagate subdiffractively over distances much larger than the Rayleigh length [7]. One of the most spectacular manifestations of filamentation is conical emission, *i.e.* the generation of new wavelengths propagating along a cone with the cone angle typically increasing with increasing wavelength shift from the pump pulse. A further important feature of filamentation that is relevant for what follows is the typical pulse splitting process that leads to the formation of two daughter pulses, one traveling slightly slower, the other slightly faster than the input Gaussian pulse.

In this letter we present a dielectric analogue based on the RIP induced by ultrashort laser pulse filamentation. We analyze in detail the light-ray geodesics predicted for such a system and show that these lead to a conical emission that is described by the same relation predicted by other models. This is verified experimentally in the present work both for a narrow bandwidth probe pulse and for a spectrally broad pulse. In the latter case a blue-shifted and a red-shifted spectral peak appear and this is

(a) E-mail: daniele.faccio@uninsubria.it

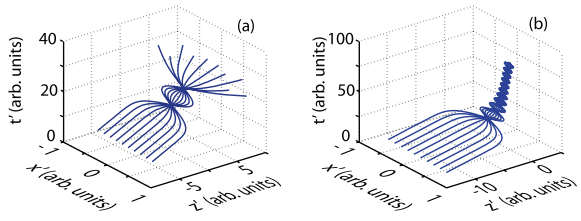

Fig. 1: (Colour on-line) (a) Spacetime light ray geodesics in the reference frame of the moving RIP. Panel (a) corresponds to a subluminal RIP: the light rays catch up with the RIP and the geodesics are deformed from the initial "straight" propagation. After two refocusing cycles (the details depend on the initial conditions) the light rays finally escape from the RIP with modified angles and frequencies. Panel (b) corresponds to an RIP with $v = c/(1+\delta n_0)$: the light rays are now trapped by the RIP event horizon and cannot escape. The increasing steepness of the curves as they approach $z = 0$ tells us that light is grinding to a halt inside the RIP.

interpreted as evidence of the complex Doppler effect [8,9]. Finally we propose possible operating conditions for the observation of Hawking radiation.

We start by analyzing how the filament modifies the effective spacetime geometry as seen by light rays. The intense core of the filament excites, through the nonlinear Kerr effect, a refractive index profile $n(x,y,z,t) = n_0 + \delta n(x,y,z,t)$, where $\delta n(x,y,z,t) = n_2 I(x,y,z,t)$, n_2 is the nonlinear Kerr coefficient and $I(x,y,z,t)$ is the intensity profile of the filament light pulse. We note that here z is the pulse longitudinal coordinate directed along the propagation direction and t is the time in the laboratory reference frame. The analogue spacetime metric in the laboratory reference frame has been deduced in the eikonal approximation for the case of a moving medium [10],

$$\mathrm{d}s^2 = \frac{c^2}{n(x,y,z,t)^2}\mathrm{d}t^2 - \mathrm{d}x^2 - \mathrm{d}y^2 - \mathrm{d}z^2 = g_{\mu\nu}\mathrm{d}x^\mu \mathrm{d}x^\nu. \tag{1}$$

The same metric holds true in our case (as will be shown in detail in a future publication), in the same approximation, even though strictly speaking here the dipoles constituting the medium, and thus the medium as a whole is at rest in the laboratory. Rather, it is only the RIP that is in movement. The null geodesics in the laboratory reference frame are the solutions of the geodesic equation $\ddot{x}^\mu + \Gamma^\mu_{\nu\sigma}(x(\lambda))\dot{x}^\nu\dot{x}^\sigma = 0$ with $g_{\mu\nu}(x(\lambda))\dot{x}^\mu(\lambda)\dot{x}^\mu(\lambda) = 0$ and $\Gamma^\mu_{\nu\rho} = (1/2)g^{\mu\sigma}[\partial_\nu g_{\sigma\rho} + \partial_\rho g_{\sigma\nu} - \partial_\sigma g_{\nu\rho}]$. Figure 1(a) shows the calculated geodesics in the RIP co-moving reference frame, considering a refractive index perturbation profile in the form of a Gaussian, $\delta n = \delta n_0 \exp[-(z - vt)^2 - x^2 - y^2]$. The RIP bends the geodesics toward its center and introduces also a time deformation. This leads to a simultaneous modification of the light ray propagation angle θ and frequency, ω. These effects are best studied in the (θ,ω)-space. We start from the incoming light ray wave vector which may be written in the RIP co-moving reference frame as $k_{\mathrm{in}} = (k^{0'}_{\mathrm{in}}, 0, 0, k'_{\mathrm{in}})$. The spacetime metric experienced by the observer co-moving with the filament is

$$\begin{aligned}\mathrm{d}s^2 &= c^2\left(1 + \left[\frac{1}{n^2} - 1\right]\gamma^2\right)\mathrm{d}t'^2 + 2\gamma^2 v\left[\frac{1}{n^2} - 1\right]\mathrm{d}t'\,\mathrm{d}z' \\ &\quad - \left(1 - \left[\frac{1}{n^2} - 1\right]\gamma^2\frac{v^2}{c^2}\right)\mathrm{d}z'^2 - \mathrm{d}x'^2 - \mathrm{d}y'^2 \\ &= g'_{\mu\nu}\mathrm{d}x'^\mu \mathrm{d}x'^\nu, \end{aligned} \tag{2}$$

where $\gamma = 1/\sqrt{1-(v/c)^2}$.

Note that in this frame the metric is stationary, being independent of the coordinate t'. Then, time translations are symmetries and determine a conserved quantity: $E = k'^\mu \xi'^\nu g'_{\mu\nu}$, where $\xi' = (1,0,0,0)$ is the associated Killing vector. Thus $E = k'^\mu g'_{\mu 0} = k'_0$ and $E_{\mathrm{out}} = E_{\mathrm{in}}$ is equivalent to

$$k'_{0\mathrm{out}} = k'_{0\mathrm{in}}. \tag{3}$$

In other words in the comoving frame the frequency is constant along a geodesic, as expected ($\omega' = ck'_0$). Turning back to the laboratory frame, where $k_{\mathrm{in}} = (k_{0\mathrm{in}}, 0, 0, -k_{\mathrm{in}})$ and $k_{\mathrm{out}} = (k_{0\mathrm{out}}, -k^x_{\mathrm{out}}, -k^y_{\mathrm{out}}, -k^z_{\mathrm{out}})$, eq. (3) becomes

$$k^z_{\mathrm{out}} = k_{\mathrm{in}} + \frac{\omega_{\mathrm{out}} - \omega_{\mathrm{in}}}{v}. \tag{4}$$

Finally, the (θ,ω) distribution of the outgoing light rays as measured in the laboratory reference frame is given by inserting eq. (4) in $\theta \simeq k_\perp/k(\omega) = \sqrt{1 - [k_{z\mathrm{out}}/k(\omega)]^2}$, where $k(\omega)$ is the material dispersion relation. We underline that this last equation, along with eq. (4), is identical to that derived within the framework of the effective-three-wave-mixing (ETWM) and X-wave models that have been successfully used to describe the main spectral features and dynamics of ultrashort laser pulser filamentation [11–16]. The present derivation of these relations on the one hand lends further support and understanding to these interpretations of dynamics in nonlinear optics. On the other hand, it justifies our analogue model as a candidate to study the analogue gravity. It is also important to note that eq. (4) has been derived under the approximation of negligible material dispersion *within* the RIP. We have verified that this approximation is valid as long as the difference between the RIP velocity, v and the material group velocity, $v_g = \mathrm{d}k/\mathrm{d}\omega$, is small. A more detailed discussion regarding this point will be given in a future publication but, as verified below, filamentation is indeed characterized by $|(v - v_g)/v_g| \ll 1$, thus justifying our derivation.

We underline that one of the cardinal points in deriving eq. (4) is the Doppler shift that allows to transform back and forth between the two reference systems. On the basis of this, two different regimes may be highlighted depending on how one accounts for the material dispersion in the medium surrounding the RIP. If we neglect the material dispersion, *i.e.* $k(\omega) = \omega n(\omega_{\mathrm{in}})/c$, we obtain the solid curve in fig. 2(a). This is equivalent to the standard

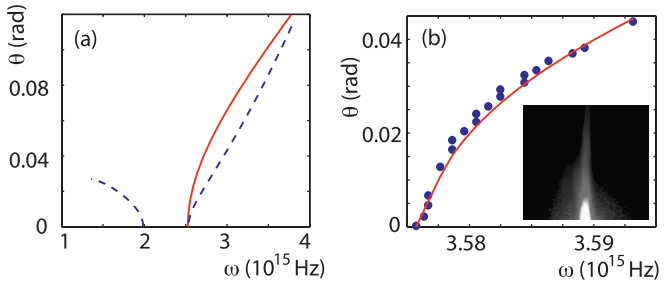

Fig. 2: (Colour on-line) (θ, ω) spectrum of the scattered light rays calculated from eq. (4). (a) Solid line: neglecting material dispersion (equivalent to the standard Doppler effect), dashed line: including material dispersion (equivalent to the complex Doppler effect). (b) Measured spectral deformation of a probe pulse in the presence of a filament. Circles: experimental maximal-intensity points taken from the measurement shown in the inset. Solid line: fit obtained using eq. (4), neglecting material dispersion.

Doppler effect in which observers at an angle with respect to the direction of motion of a scatterer experience a sweep in the scattered frequency. However, along the line of motion, no frequency shift in the *forward* direction is observed. Conversely, we may fully account for material dispersion, *i.e.* $k(\omega) = \omega n(\omega)/c$. In this case we obtain the dashed curve in fig. 2(a). This is equivalent to the so-called complex Doppler effect [8] in which the emitter is seen to emit two (or more) frequencies along the direction of motion. Indeed, in the presence of dispersion the Doppler formula $\omega' = \gamma\omega[1 - vk(\omega)]$, which lies at the basis of the coordinate transformations used in deriving eq. (4), may have two or more solutions depending on the complexity of the $k(\omega)$ dispersion relation [8,9].

We experimentally verified these findings. More explicitly, we show that a description in terms of photon spacetime geodesics, as described above, does indeed lead to a correct description of the observed experimental features. This does not necessarily imply the formation of a true event horizon in these specific settings, but it does highlight the correctness of our approach and therefore of the existence of an effective spacetime metric which may be used in future experiments, in combination with superluminal pulse propagation (in the sense that the laser pulse group velocity must be larger than the generated photon phase velocity), to investigate for example the generation of Hawking radiation.

Experiments were carried out using a regeneratively amplified Nd:Glass laser delivering pulses at 10 Hz repetition rate with 1 ps pulse duration and 1055 nm central wavelength (Twinkle, Light Conversion Ltd., Lithuania). The nonlinear Kerr medium was a 2 cm long fused-silica sample. A filament was generated by focusing down to a 100 μm input diameter a pulse with an input energy of 20 μJ. A second probe pulse is obtained by loosely focusing (1 mm diameter) 100 nJ at the second-harmonic wavelength, thus allowing to easily distinguish the pump and probe pulses. This allows one to easily separate the

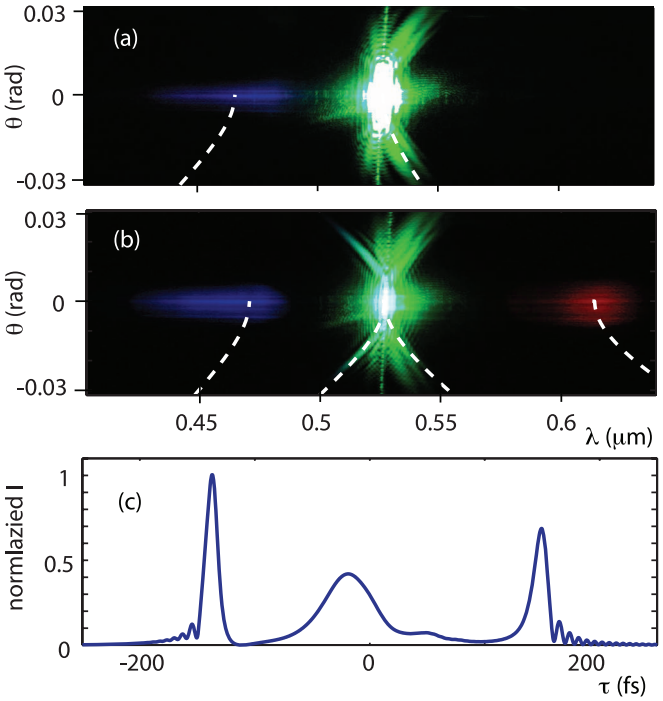

Fig. 3: (Colour on-line) (θ, λ) spectra of filament pulses in a 3 cm fused-silica sample. (a) Input energy = 1.5 μJ, (b) input energy = 1.8 μJ. The dashed lines correspond to the spectral supports predicted by eq. (4), including material dispersion and with (a) $v = 0.996c/n_g$ and (b) $v = 1.0032c/n_g$, $v = 0.997c/n_g$. (c) Numerically simulated temporal profile of the filament.

filament and probe pulses at the sample output. In fig. 2(b) the solid circles show points of maximal intensity taken from the measured output probe spectrum (shown in the inset). Due to the limited spectral bandwidth of the probe pulse we may effectively neglect material dispersion and thus obtain a good fit for the data with eq. (4), using $k(\omega) = \omega n(\omega_{\rm in})/c$.

In order to test the validity of eq. (4) in the presence of material dispersion we performed a second set of experiments in which the pulse probing the RIP is the same pump pulse generating the filament. This situation is slightly different from the first experiment in which a separate probe pulse was used. It is well-known that filamentation will lead to pulse splitting and to significant pulse shortening [7]. Starting from an input 200 fs pump pulse at the second harmonic of our laser, *i.e.* at 527 nm, the filament dynamics lead to pulse durations as short as 20–30 fs with correspondingly broad spectral bandwidths.

It is important to note that the filament is characterized by pulse splitting, *i.e.* the input, single peaked, Gaussian pulse splits into two daughter pulses. Figure 3(c) shows an example of this pulse splitting. Moreover, as they propagate, these two daughter pulses tend to increase their relative distance. In other words, in the reference frame of the input Gaussian pulse, the leading daughter pulse has a velocity v that is greater than the input Gaussian v, while the trailing daughter pulse has a v that is smaller than the input Gaussian v. Hence we

have to consider that in reality the filament creates two separate RIPs that propagate in the medium with two different velocities. The input pulse was focused to a $100\,\mu$m diameter at the input of a 3 cm long fused-silica sample. By carefully controlling the input energy it was possible to shift the onset of filamentation toward the end of the sample so that only a very short filament was observed before the pulse exited into air, thus quenching all nonlinear effects and subsequent interactions. In this way we avoid the relatively intense on-axis frequency continuum generated by long-scale filaments that would completely cover the spectral features that we are aiming to unveil. Figure 3(a) shows the measured spectrum with an input energy of $1.5\,\mu$J. The input Gaussian pump pulse spectrum has been reshaped by the RIP and exhibits marked red-shifted conical emission tails and a new blue-shifted component, mainly concentrated around $\theta = 0$. The dashed lines show the spectral support predicted from eq. (4) with $v = 0.996c/n_g$, where $n_g = c/v_g$ is the material group index at 527 nm. The observed spectral features are well reproduced by the curve and we may thus interpret the spectrum as a manifestation of the complex Doppler effect by which the input 527 nm pulse is scattered by an RIP that is traveling slightly slower than the input Gaussian pulse. We note that a similar blue-shifted peak has been previously reported [17] and was shown to be related to a steep trailing front within the filament. This is also in keeping with the results and interpretation of Philbin *et al.*, who assimilate a trailing pulse edge to the analogue of a white hole [6]. This may be intuitively understood by considering that, for example along the z axis, the horizon is defined by the condition $c = n(z_h)v$. For a Gaussian-shaped pulse in a dispersionless medium, this condition is met in two points, one at leading edge, z_+, and the other at the trailing edge, z_-, of the pulse. These are the points where photons are at rest relative to the pulse. On the trailing edge the pulse has a positive slope so that c/n decreases and the photon cannot pass through z_-. In other words, light cannot enter the RIP from z_-, just as for a white-hole horizon. In z_+ the pulse has a negative slope and the same argument shows that then only photons in $z > z_+$ can escape the pulse. This is the analogue of a black-hole horizon. for a real medium, dispersion implies that such a scenario is true only for a certain range of frequencies and the position of the horizons themselves may depend on the frequency.

The geodesics shown in fig. 1 refer precisely to the interaction of light rays with the trailing edge of the RIP. In the presence of a true event horizon, as in fig. 1(b), the light rays will accumulate at the horizon with a continuously increasing compression of the wavelength, *i.e.* an ever-increasing blue-shift in the spectrum. In the absence of a true event horizon, that is in the case in which the geodesics are not trapped but, rather, simply deformed by the RIP, the light rays will still be blue-shifted albeit to a lesser degree, as observed in our measurement.

Figure 3(b) shows the measured spectrum with a slightly higher input energy of $1.8\,\mu$J. Now, in addition to the blue-shifted peak, we also observe a red-shifted peak. As before, the dashed lines show the spectral support predicted from eq. (4), with $v = 0.997c/n_g$ for the blue-shifted spectrum and with $v = 1.0032c/n_g$ for the red-shifted spectrum. The fact that the blue peak may appear independently of the red peak excludes four-wave mixing as the generating process. Indeed, the four-wave–mixing phase-matching relations imply that two pump photons will give rise to the simultaneous formation of one signal (blue) photon and one idler (red) photon. It is not possible to ensure this four-wave–mixing process if this elementary energy conservation is not preserved. We thus interpret the on-axis red peak as the result of the complex Doppler effect for light rays scattered from a leading front in the filament. This leading front is just a time-reversed realization of the trailing front analyzed in fig. 3(b) and it may thus be assimilated to a black hole [6]. In fig. 3(c) we show the numerically calculated intensity profile of the pulse along the propagation axis at the sample output. A description of the numerical code is given in [11,18,19] and a detailed comparison with experiments is given in [17]. As can be seen, the pulse is indeed characterized by a sharp trailing edge, that gives rise to a blue-shifted spectral peak, and by an equivalently sharp leading edge that gives rise to red-shifted spectral peak. For different input energies the filament dynamics may change significantly and only a trailing pulse (and blue-shifted spectral peak) may be observed [17], thus explaining the difference between figs. 3(a) and (b). We note that for a pulse propagating in nonlinear media with a positive Kerr coefficient, the formation of a shock front on the trailing edge is to be expected and has been frequently reported [20,21]. However the formation of a leading shock front is not as obvious and indeed is a peculiar feature of filamentation [22]. This aspect makes filamentation particularly suited to the study of what concerns the present work.

We underline once more that in order to actually observe Hawking radiation the RIP should travel superluminally with respect to the phase velocity of the incoming light rays. Figure 1(b) shows the geodesics in the co-moving RIP reference frame in the limiting case for the horizon event formation, *i.e.* for an RIP velocity equal to the light phase velocity. The geodesics are now strongly deformed and, as light gradually grinds to a halt, cannot escape from the RIP. From the experimental viewpoint, fig. 3(c) shows how the filament pulse (and thus also the corresponding RIP) consists of two main peaks, with the trailing peak being slower and the leading peak faster than the input pulse. It has been shown that by correctly choosing the input pulse conditions in function of the specific Kerr medium, it is possible to create a leading pulse that is superluminal even with respect to the same input carrier frequency [23]. Such an RIP will therefore appear as a black hole for the pump pulse carrier frequency.

In conclusion we have described the spacetime geometry of light rays in the presence of a filament. The equations predict a specific shape for the aberrated light rays that has been confirmed experimentally. The results indicate the presence of both white and black-hole horizons. Using the same formulas of [6], a 5 fs pulse at 800 nm (2 optical cycles) will lead to a Hawking temperature corresponding to a peak wavelength around 1.2 μm for which high sensitivity detectors are readily available. One may envision other possibilities for achieving superluminal pulses in Kerr media such as the use of Bessel-like pulses, although filaments maintain a certain attractiveness due to the spontaneous pulse shortening and the possibility to observe more exotic phenomena such as black-hole lasing [24,25].

The experiments presented here may certainly be described by "standard" filamentation models such as that presented in [17]. We point out that the aim of this work is to show that already-known physics may be re-interpreted in terms of metrics and geodesics, *i.e.* using the formalism of general relativity. This thus gives us the grounding to propose filamentation as a valid analogue gravity model with which to attempt more adventurous experiments aimed, for example, at the first observation of Hawking radiation.

* * *

The authors acknowledge measurements performed in the Ultrafast Nonlinear Optics Laboratory, Università dell'Insubria, Como, Italy, led by Prof. P. Di Trapani. JVM acknowledges support from US Air Force Office of Scientific Research (AFOSR) under contract FA9550-07-1-0010.

REFERENCES

[1] Birrell N. D. and Davies P. C. W., *Quantum Fields in Curved Space* (Cambridge University Press, Cambridge, England) 1984.
[2] Hawking S. W., *Commun. Math. Phys.*, **43** (1975) 199.
[3] Unruh W. G., *Phys. Rev. Lett.*, **46** (1981) 1351.
[4] Novello M. *et al.* (Editors), *Artificial Black Holes* (World Scientific, Singapore) 2002.
[5] Barceló C. *et al.*, *Living Rev. Relativ.*, **8** (2005) 12.
[6] Philbin T. G. *et al.*, *Science*, **319** (2008) 1367.
[7] Couairon A. *et al.*, *Phys. Rep.*, **441** (2007) 47.
[8] Frank I. M., *Science*, **11** (1960) 131.
[9] Sorokin Yu. M., *Radiophys. Quantum Electron.*, **36** (1993) 410.
[10] Leonhardt U. *et al.*, *Phys. Rev. A*, **60** (1999) 4301.
[11] Kolesik M. *et al.*, *Opt. Express*, **13** (2005) 10729.
[12] Faccio D. *et al.*, *Opt. Express*, **15** (2007) 13077.
[13] Kolesik M. *et al.*, *Phys. Rev. Lett.*, **92** (2004) 253901.
[14] Conti C., *Phys. Rev. E*, **70** (2004) 046613.
[15] Faccio D. *et al.*, *Phys. Rev. Lett.*, **96** (2006) 193901.
[16] Averchi A. *et al.*, *Opt. Lett.*, **33** (2008) 3028.
[17] Faccio D. *et al.*, *Phys. Rev. A*, **78** (2008) 033825.
[18] Kolesik M. *et al.*, *Phys. Rev. Lett.*, **89** (2002) 283902.
[19] Kolesik M. and Moloney J. V., *Phys. Rev. E*, **70** (2004) 036604.
[20] DeMartini F. *et al.*, *Phys. Rev.*, **164** (1967) 312.
[21] Alfano R. R., *The Supercontinuum Laser Source,* (Springer-Verlag, New York) 1989.
[22] Bragheri F. *et al.*, *Phys. Rev. A*, **76** (2007) 025801.
[23] Faccio D. *et al.*, *Opt. Express*, **16** (2008) 11103.
[24] Corley S. *et al.*, *Phys. Rev. D*, **59** (1999) 124011.
[25] Leonhardt U. *et al.*, in *Quantum Analogues: From Phase Transitions to Black Holes and Cosmology* (Springer, Berlin) 2007.